Microclimate and forest density drive plant population dynamics under climate change

Pieter Sanczuk, Karen de Pauw, Emiel de Lombaerde, Miska Luoto, Camille Meeussen, Sanne Govaert, Thomas Vanneste, Leen Depauw, Jörg Brunet, Sara Cousins, et al.

Microclimate and forest density drive plant population dynamics under climate change

Pieter Sanczuk[1*], Karen De Pauw[1], Emiel De Lombaerde[1], Miska Luoto[2], Camille Meeussen[1], Sanne Govaert[1], Thomas Vanneste[1], Leen Depauw[1], Jörg Brunet[3], Sara A.O. Cousins[4], Cristina Gasperini[5], Per-Ola Hedwall[3], Giovanni Iacopetti[5], Jonathan Lenoir[6], Jan Plue[7], Federico Selvi[5], Fabien Spicher[6], Jaime Uria-Diez[3], Kris Verheyen[1], Pieter Vangansbeke[1], Pieter De Frenne[1]

[1]Forest & Nature Lab, Department of Environment, Faculty of Bioscience Engineering, Ghent University, Geraardsbergsesteenweg 267, 9090 Melle-Gontrode, Belgium

[2]University of Helsinki, Department of Geosciences and Geography, Gustaf Hällströmin katu 2, 00014 Helsinki, Finland

[3]Southern Swedish Forest Research Centre, Swedish University of Agricultural Sciences, Box 190, 234 22 Lomma, Sweden

[4]Landscapes, Environment and Geomatics, Department of Physical Geography, Stockholm University, Svante Arrhenius väg 8, 106 91 Stockholm, Sweden

[5]Department of Agriculture, Food, Environment and Forestry, University of Florence, P. le Cascine 28, 50144 Florence, Italy

[6]UMR CNRS 7058 “Ecologie et Dynamique des Systèmes Anthropisés” (EDYSAN), Université de Picardie Jules Verne, 1 Rue des Louvels, 80000 Amiens, France

[7]IVL Swedish Environmental Institute, Stockholm, Sweden

*Corresponding author: Pieter Sanczuk

Email: Pieter.Sanczuk@UGent.be

Abstract

Macroclimatic changes are impacting ecosystems worldwide. The majority of terrestrial species, however, lives in the shade of trees where impacts of macroclimate change are buffered. Yet, how microclimate buffering can impact future below-canopy biodiversity redistributions at the continental scale is unknown. Here we assess the effects of changes in microclimate and forest density on plant population dynamics under macroclimate change. We built 25-m resolution mechanistic demographic distribution models at European extent based on plant demography responses to changes in the environment in a unique cross-continental climate change transplant experiment. We show that changes in microclimate and light due to canopy opening amplify macroclimate change impacts on forest biodiversity, while shady forest floors due to dense tree canopies mitigate severe warming impacts. The microclimate and forest density thus emerge as powerful tools for forest managers and policy makers to shelter forest biodiversity from climate change.

Key words

Climate change experiment, demography, integral projection model, forest, microclimate, transplant experiment, species distribution, understorey.

Main

Numerous species are shifting their distributions towards higher elevations and latitudes due to the warming of the climate system[1–3]. Predictive models that quantify range shifts under climate change almost exclusively rely on projected free-air macroclimatic conditions. Macroclimate data are estimated from weather stations that record free-air temperatures at 1.5 to 2 m above short grass, thereby failing to describe the relevant microclimatic conditions that are experienced by the majority of terrestrial species on Earth[4]. Moreover, microclimatic conditions are highly variable at fine spatial grains (typically 100 m to much finer) while macroclimate data are generally only available at a coarse resolutions (typically 1 km or coarser)[5]. To date, piling evidence points towards the importance of microclimatic and other fine-grained environmental conditions for species' range shifts under climate change[6–12]. If we are to improve our predictive accuracy on future range dynamics, we cannot ignore this important part of the environment[13].

In forests, directional changes towards species adapted to warmer temperatures remain somewhat elusive, with slower, absent or even disparate trends frequently observed[7,8]. For instance, many forest communities are lagging behind predictions based on macroclimatic temperature increases[7,14–16]. Next to slow species' demography and dispersal rates[17,18], these 'climatic lags' are attributed to processes operating at fine spatial grains.

Due to their highly complex structure, trees are ecosystem engineers that attenuate variation in below-canopy climatic conditions (i.e. the forest microclimate) and buffer forest species from macroclimatic temperature extremes[19–22]. Microclimates determine major forest ecological processes such as nutrient cycling[23], evapotranspiration[24], tree regeneration[25], soil seed bank composition[26] and understorey species range dynamics[15,27,28].

64 The capacity of forests to buffer below-canopy temperature fluctuations is highly heterogenous
65 in space and time, and inherently links to forest structural complexity, forest density and distance
66 to the forest edge: simple-structured forests and forest edges usually have less buffered
67 microclimates[19,21] and these conditions typically result in community reordering towards tall,
68 competitive and warm-affinity generalists[16,29–31]. However, how and to what extent fine-grained
69 forest microclimates determine understorey plant responses to climate change across a large
70 geographic extent remains an open question[32]. The relevance of considering forest microclimates
71 is further enhanced since climate change has now initiated the largest pulse of forest disturbances
72 and canopy opening in at least 170 years in Europe[33,34], which takes away a line of defence of
73 below-canopy biodiversity.
74
75 Here we designed a unique continental-scale transplant experiment along the entire latitudinal
76 gradient of the European temperate broadleaved forest biome. Using an integral projection
77 modelling (IPM) framework, we integrated the data to build mechanistic demographic
78 distribution models (DDMs) at 25 m resolution. DDMs allow to predict mechanistically-
79 informed range-wide population dynamics based on the responses of demographic vital rates of a
80 species' life cycle (that is, survival, growth and reproduction) to changes in the environment. In
81 contrast to the widely used species distribution models[35], DDMs facilitate the integration of
82 biologically relevant mechanisms at ecologically meaningful spatial scales via experimental
83 research[36,37].
84
85 Both manipulative experiments (experimentally changed environmental conditions where species
86 live) and transplant experiments (translocation of species towards new environments) are

87 frequently applied to unravel plant responses to changing environmental conditions[29,30,38,39].
88 Especially when replicated at fine spatial grains (e.g. < 100 m) across several locations covering
89 a large spatial extent (e.g. > 1,000 km), such experiments are particularly suited to understand of
90 the effects of environmental drivers in a biogeographical context[40]. We established transplant
91 experiments in five contrasting biogeographical areas along a *c.* 1,750 km latitudinal gradient,
92 and along two crossed microclimate gradients driven by forest structure and distance to the forest
93 edge (Methods; Fig. 1a,b). In three of the geographic regions, additional experimental heating
94 (simulating macroclimate warming using infrared heaters) and irradiation (simulating forest
95 canopy opening using fluorescent tubes) treatments were applied in a full-factorial design
96 (Methods; Fig 1c, Extended Data Fig. 1). Integrating the demographic data from the transplant
97 experiment, DDMs were parameterized to project the current and future distributions of common
98 understorey plant species, taking into account the effects of forest microclimate and forest cover
99 density.
100
101 Methodologically, we focused on a set of twelve common understorey plant species native to
102 European broadleaved forests, selected along a forest specialist – generalist spectrum inferred
103 from the Colonization Capacity Index (CCI)[41]. The species can thus be expected to respond
104 differently to macroclimatic and microclimatic gradients. We transplanted 8,064 individuals into
105 mesocosm communities that were stratified assemblages of four species from contrasting
106 ecological groups. A total of 25,997 *in situ* demographic measurements across six vital rates
107 (survival probability, growth rate, flowering probability, number of flowers, number of seeds and
108 seedling sizes) were regressed against plant size – describing each individual's state[42] – and the
109 environment using mixed-effect models (Methods). The vital rate models were integrated into

IPMs to infer the effect of the environment on population dynamics[43]. Demography-based distribution maps for each species were generated by projecting the IPMs across the study area (i.e. a broad window around the European temperate broadleaved forest biome) under all combinations of current and future macroclimatic conditions and forest cover density scenarios (following the protocol of [36,37]). Projections of the DDMs under future macroclimatic conditions were produced for the period 2070 (i.e. the average macroclimate over the period 2061 – 2080) for the worst-case climate scenario (i.e. representative concentration pathway [RCP] 8.5). Projections of the DDM under forest cover density scenarios were based on changes in the current forest cover density (from minus 50% to plus 50%). In all model predictions, we assumed temperature offsets to stay constant over time.

Plant vital rate responses

Across all species, plant size and the environmental variables predicted a substantial part of the variation in the vital rates (average marginal R^2 = 0.33; average conditional R^2 = 0.43; Fig. 2; Supplementary Table 1). Among all vital rates, the macroclimate variables growing-season temperature and precipitation were strong predictors of the individual's survival probability (after model selection, growing-season temperature and precipitation was included in the vital rate models of survival of respectively ten, and nine focal species), and in general suggested lower plant survival in colder and dryer macroclimatic conditions (Fig. 2). Since Darwin's essay 'On the origin of species', abiotic stress brought about by e.g. harsh climatic conditions has been postulated to dominate poleward (in latitude) and upward (in elevation) limits of species ranges[44]. This pattern has already been generally validated[45–47], and our results seem to mirror this pattern (but see [48–50]). In line with a similar approach in a South African shrub species[36], our

results furthermore suggest that distribution patterns in the focal species are predominantly driven by hampered survival rather than reduced growth or fecundity.

Also local environmental conditions typically variable at fine spatial grains have been postulated to drive range dynamics across broad spatial extents[48,50,51]. Biotic interactions, for example, were shown to affect range limits through cumulated stress induced by harsh macroclimatic conditions and competition[10,12]. Likewise, environmental stress induced by unfavourable forest microclimates can possibly alter range dynamics in forest species[32], but this remained untested. Our results indeed hint towards the importance of forest microclimatic conditions (in terms of summer and winter temperature offsets), and forest cover density on multiple vital rates that contribute to population growth. Interestingly, in contrast to the macroclimate variables, forest microclimate variables had strong effects on several vital rates from which the direction of the effect was dependent on the species' specialism to forests. Among all vital rates, this pattern was again the most pronounced for survival probability (after model selection, summer and winter temperature offsets, and forest cover density was included in the vital rate models of survival of eight, nine, and nine focal species, respectively; Fig. 2).

Typical forest specialists had the highest survival probability when winter minima (i.e. more positive winter temperature offset values) and summer maxima (i.e. more negative summer temperature offset values) were buffered below tree canopies (Fig. 2; Supplementary Table 4). In contrast, the survival probability of forest generalist species responded to a lesser extent to buffered temperature extremes but were negatively affected by high forest cover density, possibly because these species lack physiological adaptations to cope with low light levels[52]. For

example, based on our data, we estimated that, on average, an increase of the thermal buffering during summer from -1°C to -2°C (i.e. what is typically observed along a 100 meter forest edge to interior transect[21]), resulted in a 37% increase in the survival probability in *Oxalis acetosella*, a typical forest specialist, but only in an 11% increase in the survival probability in *Urtica dioica*, a fast-colonizing generalist (Extended Data Fig. 7). Similarly, an increase of the forest cover density from 50% to 60% resulted in a 13% higher survival probability in *Anemone nemorosa*, another emblematic forest specialist in temperate Europe, but a 6% lower survival probability in the generalist *Urtica dioica*. Naturally, forest managers cannot manipulate the forest cover density (and thus light availability) without altering the subcanopy temperature offsets as both are linked and jointly determine the specific microclimatic conditions that are experienced by understorey species. Nevertheless, managers can strive to a specific set of microclimatic conditions (e.g. shady forest-floor conditions that are buffered from free-air temperature extremes through maintaining a high canopy cover), hereby deploying microclimates as a tool to "manipulate" species' turnover in understorey plant communities.

Demographic distribution model predictions

Integrating the effects of the local and regional environmental drivers on all vital rates that contribute to the generative population growth allowed us to project the population growth rate (λ) across Europe (Fig. 3; Extended Data Fig. 12 for geographic uncertainty of λ). We generated mechanistically-informed distribution maps at 25 m resolution for the extent of temperate Europe. As expected from the vital rate models (Fig. 2), the DDMs showed substantial variation in λ, both at the continental-level (area of 28 million km^2) and at the landscape-level extent (three areas of 4 km^2), indicating the importance of fine-grained microclimatic conditions (i.e. summer

179 and winter temperature offsets), and forest cover density, next to the coarse-grained
180 macroclimatic conditions (i.e. growing-season temperature and precipitation) in driving forest
181 plant population dynamics. While evidently the variation in λ at the landscape-level represents
182 only a subtle part of the variation at the continental extent, these results highlight the
183 fundamental role of forest microclimatic conditions on the local persistence of understorey
184 populations[15].
185
186 Considerable changes were predicted in the spatial distribution for all understorey species due to
187 macroclimate change (Fig. 4; Extended Data Figs.10,11). Interestingly, and very relevant in light
188 of the accelerating rates of canopy disturbances beyond historical averages[33,53,54], we detected
189 that changes of the forest cover density (and thus altered light regimes at the forest floor) may
190 amplify macroclimate change effects on forest understorey plants. We furthermore found that
191 both the direction (positive or negative) and magnitude of the species' population responses was
192 dependent on their specialism to forests (Fig. 5, Supplementary Table 4). For example, in
193 *Anemone nemorosa*, a 50% reduction of the forest cover density would likely amplify the
194 negative impact of macroclimate change by not less than 195%. In contrast, in the generalists
195 *Alliaria petiolata* and *Urtica dioica*, beneficial effects brought about by canopy opening could
196 far exceeded the negative impacts of macroclimate change on population growth (Extended Data
197 Figs. 10,11). Mechanistically, the vital rate models suggest that forest specialist species were
198 negatively impacted by canopy opening due to higher light levels that hamper survival, likely as
199 an inevitable consequence of elevated competitive interactions with more generalist species.
200 On the contrary, an increase of the forest cover density could mitigate macroclimate change
201 impacts on forest specialist species by limiting abrupt light stress. This trend corroborates

observational data[55], and highlights the importance of a continuous cover forest management under climate change. We find, for instance, in *Anemone nemorosa* that an increase of 20% forest cover density mitigates the impacts of macroclimate change by not less than 65%, while an increase of 50% compensate almost the entire (92%) effect (Fig. 5, Extended Data Figs. 10,11). While direct impacts of macroclimate change on canopy disturbances are increasingly apparent[53] with cascading effects on understorey biodiversity[56], managers should maximally retain dense forest canopies to maintain shady forest-floor conditions to mitigate severe impacts on understorey communities. Nonetheless, to sustainably preserve diverse forest communities, policy makers should first merit key priority to tackle drivers of macroclimate change.

In all model predictions, we assumed temperature offsets to stay constant over time although forest disturbance reduces offset values[19,21] and warming enhances offset values under maintained forest cover[22]. Thus, our model predictions likely underestimated the effect of changes in the forest cover density on plant population dynamics under macroclimate change, and are thus conservative. High-resolution projected temperature offsets under climate change are indeed not yet available, and are most likely driven by a complex interplay among many environmental variables, including macroclimate and forest cover density, but also by e.g. dynamics in cloud cover[57]. Using constant temperature offset values in all future predictions, however, allowed us to isolate changes in species' demography within the community driven by the independent effect of light[30].

Challenges in demographic distribution modelling

While the mechanistic nature of DDMs brought advantages over more correlative approaches such as species distribution modelling, it also has methodological limitations that should be considered when interpreting the results. First, DDMs require us to make assumptions on the structure of the vital rate models. While more complex vital models are likely to better describe the natural complexity of the system (e.g. by including higher order polynomials and interactions terms), the robust parameterization of these models typically trades off with the number of observations in the data set. For this reason, we here only considered monotonous relationships of the vital rates to the environment, while a qualitative sensitivity analyses against this approach suggested that some vital rate models are likely to follow a more complex response curve (Extended Data Fig. 7). For instance, the vital rates survival and flowering probability in *Allium ursinum* more likely followed a unimodal response to the winter temperature offset gradient which is not captured by the assumed monotonous response curve in our models. Second, DDMs are data hungry models. Ideally, demographic data should be collected in the critical macro- and microenvironmental conditions within the study area. This is, however, often impossible due to a limitation of time and resources. Given that our work aimed to assess fine-grained variation in λ, we put maximal effort the collect demographic data in the critical microclimatic conditions, while the range of sampled macroclimatic conditions within the study area was still not fully covered (Extended Data Fig. 14). Model extrapolation is inherent to predictive ecology, and the accuracy of the presented DDM predictions (far) beyond the macroclimatic range that was sampled (in our case, e.g. at higher elevations in the Alps) is evidently lower. A well-designed plot network which *a priori* considers the goal of the study, is thus key in the efficient and successful application of DDMs.

Conclusions

In sum, we here built demographic distribution models based on mechanistic plant responses to both microclimate and macroclimate. We found that fine-grained microclimatic conditions and forest density, in addition to the macroclimatic conditions, play a fundamental role in understorey species' distributions. Our results suggest that changes in forest-floor conditions, regardless of whether the drivers of canopy opening are natural or anthropogenic, can amplify macroclimate change impacts on forest biodiversity. We propose that sustainable forest management should conserve conditions that favour the survival of forest specialist species through maintaining a high canopy cover to limit both abrupt light stress and temperature increase. The DDMs suggest that macroclimate change impacts on forest specialist species (e.g. emblematic species such as *Anemone nemorosa* and *Allium ursinum*) could be mitigated by increased forest density. Forest generalists whose ranges often promptly respond to changes in the macroclimate system, are likely to keep on taking advantage from the natural variation in microclimate and light availability after disturbance that is inherent to European broadleaved forest dynamics.

Our integrative methodological framework (R-code for the analyses of the DDMs available as Supplementary Material) is adaptable to many other species and ecosystems to examine the importance of fine-grained environmental conditions in a warming world, and can undoubtedly improve our understanding of species range dynamics under 21st century climate change.

Figures

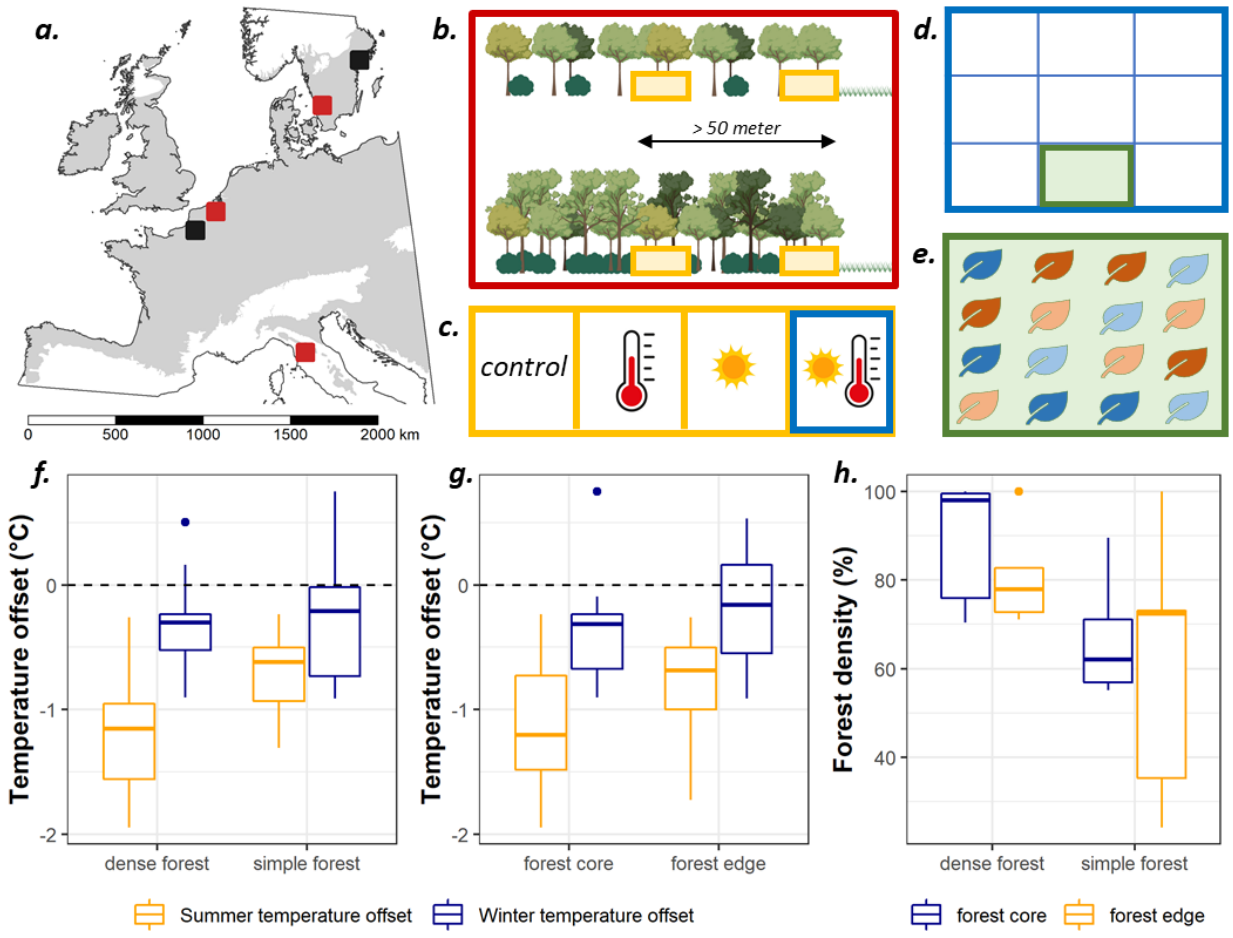

Figure 1 Overview of the study. (a) Experimental locations with heating and irradiation treatments (red), control plots (black) and the Temperate broadleaved and mixed forest biome[58] (shaded). (b) Experimental sites (yellow) along two microclimate gradients created by forest structure and forest edge distance. (c) One experimental site with heating and irradiation treatments. (d) Nine mesocosm communities per treatment. (e) A mesocosm community containing four individuals of four contrasting species. (f-g) Temperature offset values in dense *vs.* simple forests and forest cores *vs.* edges. (h) Forest cover density in dense *vs.* simple forests. In all boxplots, we present median (horizontal line), 1st and 3th quantile (lower and upper hinges, 1.5 time the inter-quartile-range (whiskers), and outliers (points).

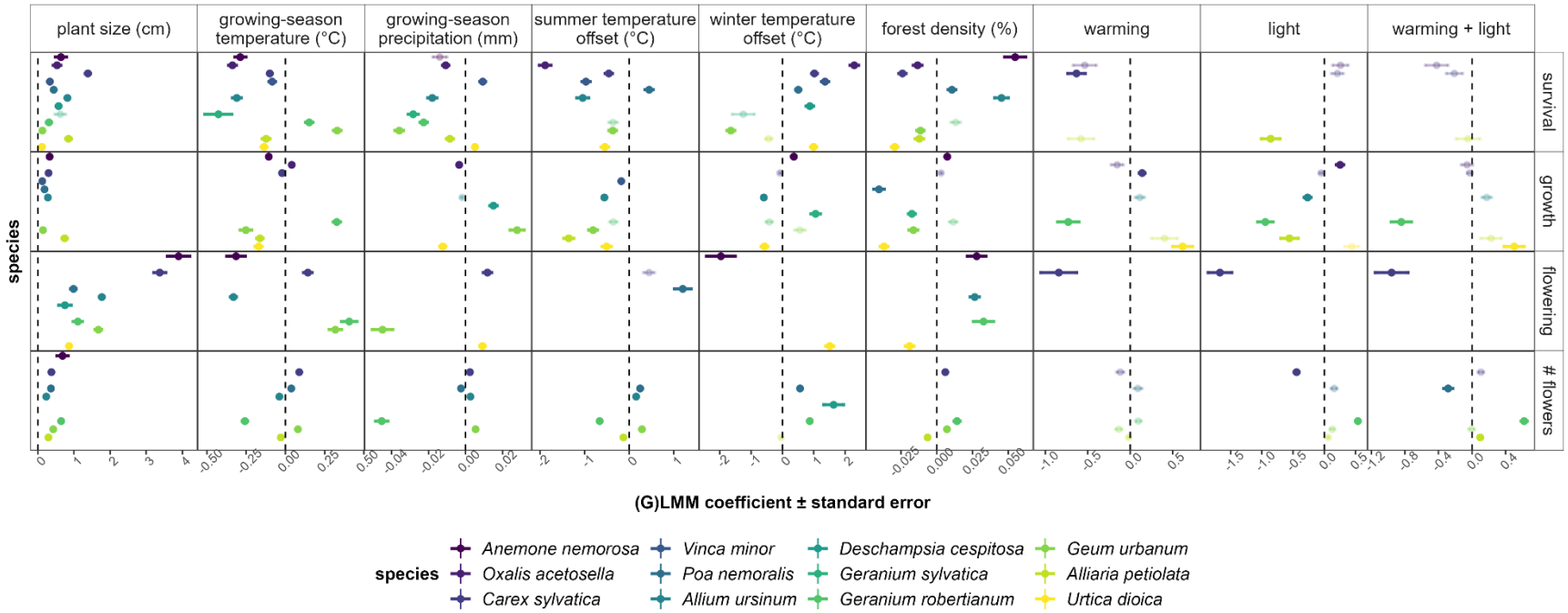

Figure 2 Four key vital rates survival probability (survival), growth rate (growth), flowering probability (flowering) and the number of flowers (# flowers) regressed against individual plant height (plant size) and the environmental covariates. Values are (generalized) linear mixed-effect model (LMM) coefficient estimates [± standard error] (after model selection; presented in horizontal way). Species are ranked following the Colonization Capacity Index (CCI). Significant effects ($p < .05$) are in bold. Non-significant effects ($p \geq .05$) are faded. Model coefficient estimates for the vital rates number of seeds and seedling size are presented in Extended Data Fig. 9. See Supplementary Table 1 for model details.

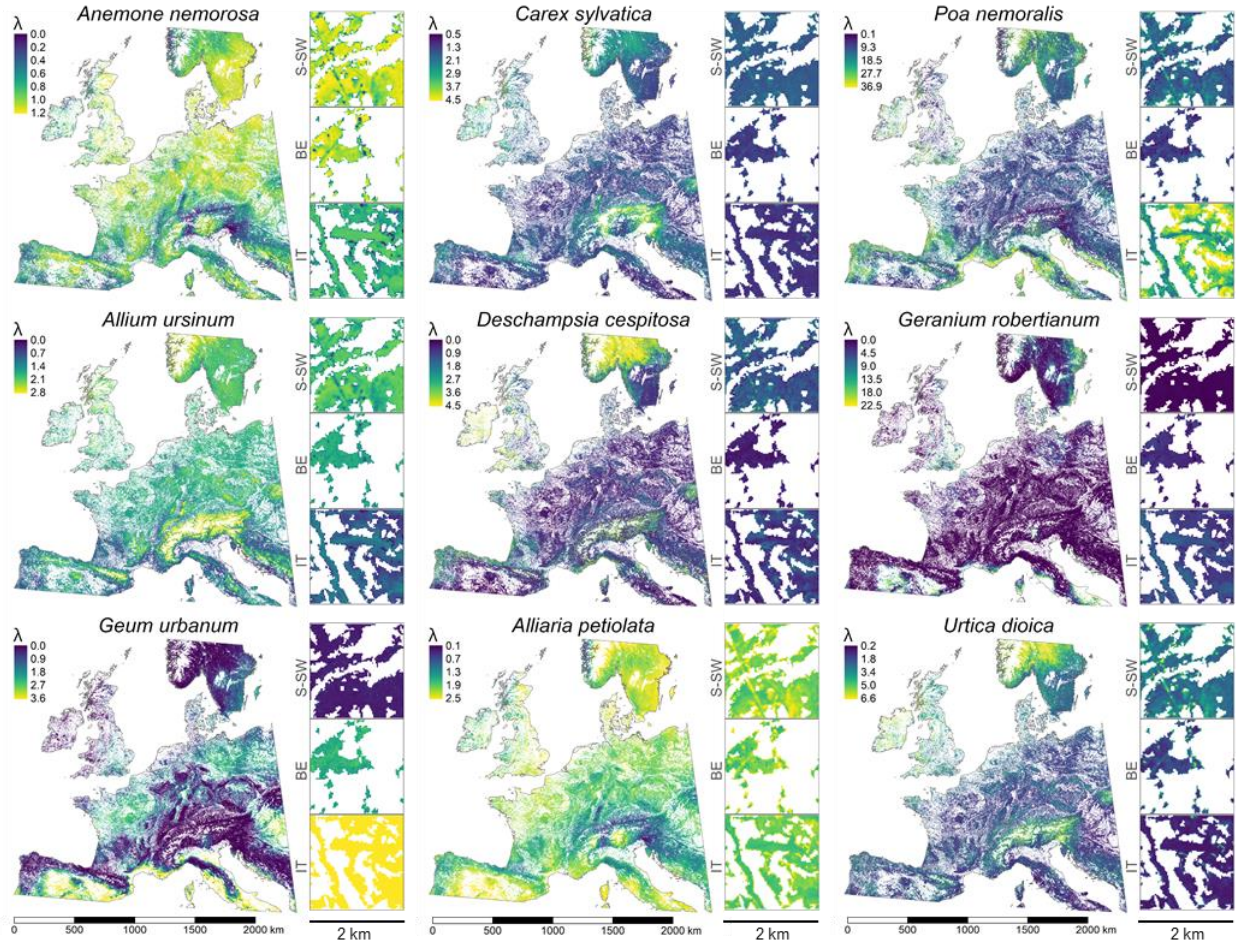

Figure 3 Range model predictions of the current distributions (estimated as the population growth rate, λ) at the continental scale and the landscape scale (three example areas of 2 × 2 km [400 ha] around the centroid of the experimental sites in Italy [IT], Belgium [BE] and South Sweden [S-SW]) based on population growth rates (λ). For three species (*Oxalis acetosella*, *Vinca minor* and *Geranium sylvaticum*), the data did not allow to construct DDMs due to the absence of observations related to fecundity. Maps are in an equal area projection [EPSG:3035].

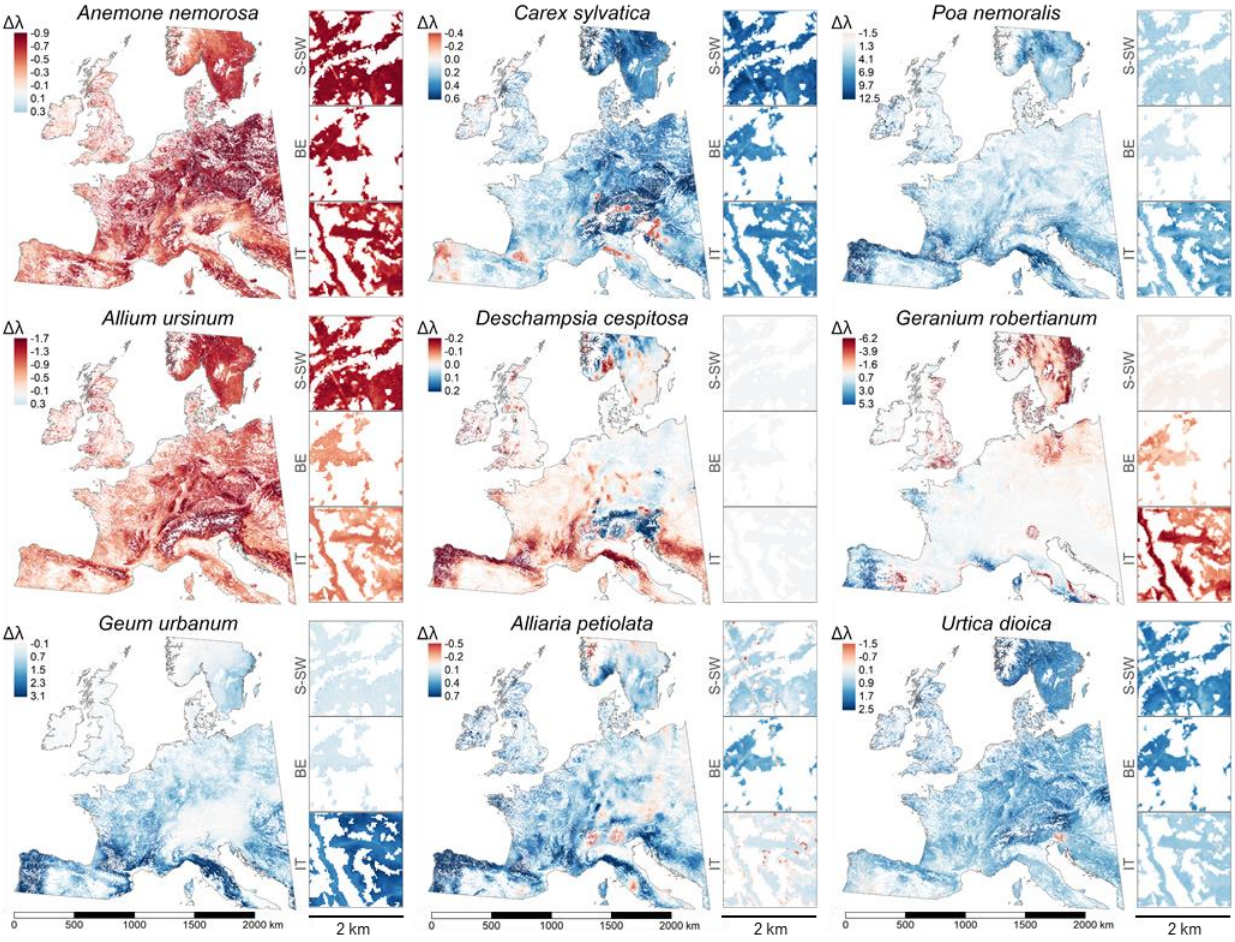

Figure 4 Predicted change in future population growth rate (Δλ) under future macroclimate change (RCP 8.5) and 50% forest density decrease at the continental scale and the landscape scale (three areas of 2 × 2 km [400 ha] around the centroid of the experimental sites in Italy [IT], Belgium [BE] and South Sweden [S-SW]). Changes are expressed relative to the range model predictions of the current distributions (Fig. 3). Maps are in an equal area projection [EPSG:3035]. See Extended data Fig. 10 for maps on all environmental change scenarios.

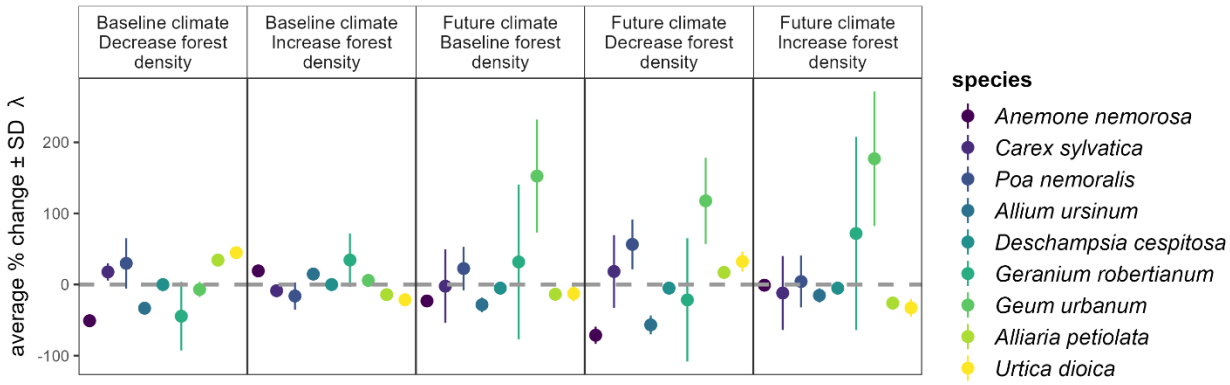

296

297 **Figure 5** Predicted change in future population growth rate (λ) for different climate and forest density
298 scenarios (50% decrease and 50% increase). Plotted are continental-scale average % change [± standard
299 deviation (SD)] in λ relative to the baseline predictions (Fig. 3) for all combinations of future
300 macroclimate change and increased and decreased forest density. Species are ranked from specialists
301 (left) to generalists (right) following their colonization capacity index (CCI).
302

References

1. Chen, I., Hill, J. K., Ohlemüller, R., Roy, D. B. & Thomas, C. D. Rapid Range Shifts of Species of Climate Warming. *Science (80-.).* **333**, 1024–1027 (2011).
2. Lenoir, J. *et al.* Species better track climate warming in the oceans than on land. *Nat. Ecol. Evol.* **4**, 1044–1059 (2020).
3. Parmesan, C. & Yohe, G. A globally coherent fingerprint of climate change impacts across natural systems. *Nature* **421**, 37–42 (2003).
4. De Frenne, P. & Verheyen, K. Weather stations lack forest data. *Science (80-.).* **351**, 234–234 (2016).
5. Lembrechts, J. J. *et al.* Comparing temperature data sources for use in species distribution models: From in-situ logging to remote sensing. *Glob. Ecol. Biogeogr.* **28**, 1578–1596 (2019).
6. De Frenne, P. *et al.* Latitudinal gradients as natural laboratories to infer species' responses to temperature. *J. Ecol.* **101**, 784–795 (2013).
7. Zellweger, F. *et al.* Forest microclimate dynamics drive plant responses to warming. *Science (80-.).* **368**, 772–775 (2020).
8. Bertrand, R. *et al.* Changes in plant community composition lag behind climate warming in lowland forests. *Nature* **479**, 517–520 (2011).
9. Suggitt, A. J. *et al.* Extinction risk from climate change is reduced by microclimatic buffering. *Nat. Clim. Chang.* **8**, 713–717 (2018).
10. Shepard, I. D., Wissinger, S. A. & Greig, H. S. Elevation alters outcome of competition between resident and range-shifting species. *Glob. Chang. Biol.* **27**, 270–281 (2021).
11. Alexander, J. M., Diez, J. M. & Levine, J. M. Novel competitors shape species' responses to climate change. *Nature* **525**, 515–518 (2015).
12. Sanczuk, P. *et al.* Competition mediates understorey species range shifts under climate change. *J. Ecolgy* 1–13 (2022). doi:10.1111/1365-2745.13907
13. Colwell, R. K. Spatial scale and the synchrony of ecological disruption. *Nature* **599**, E8–E10 (2021).
14. De Frenne, P. *et al.* Microclimate moderates plant responses to macroclimate warming. *PNAS* **110**, 18561–18565 (2013).
15. Lenoir, J., Hattab, T. & Pierre, G. Climatic microrefugia under anthropogenic climate change: implications for species redistribution. *Ecography (Cop.).* **40**, 253–266 (2017).
16. Dietz, L., Collet, C., Eric, J. D., Lisa, L. & Gégout, J. Windstorm-induced canopy openings accelerate temperate forest adaptation to global warming. *J. Biogeogr.* **29**, 2067–2077 (2020).
17. Bertrand, R. *et al.* Ecological constraints increase the climatic debt in forests. *Nat. Commun.* **7**, (2016).
18. Sanczuk, P. *et al.* Species distribution models and a 60-year-old transplant experiment reveal inhibited forest plant range shifts under climate change. *J. Biogeogr.* **49**, 537–550 (2022).
19. De Frenne, P. *et al.* Global buffering of temperatures under forest canopies. *Nat. Ecol. Evol.* **3**, 744–749 (2019).
20. Haesen, S. *et al.* ForestTemp - Sub-canopy microclimate temperatures of European forests. *Glob. Chang. Biol.* **27**, 6307–6319 (2021).
21. Meeussen, C. *et al.* Microclimatic edge-to-interior gradients of European deciduous forests. *Agric. For. Meteorol.* **311**, (2021).
22. De Lombaerde, E. *et al.* Maintaining forest cover to enhance temperature buffering under future climate change. *Sci. Total Environ.* **810**, (2022).
23. Landuyt, D. *et al.* The functional role of temperate forest understorey vegetation in a changing world. *Glob. Chang. Biol.* **25**, 3625–3641 (2019).
24. Kassuelke, S. R., Dymond, S. F., Feng, X., Savage, J. A. & Wagenbrenner, J. W. Understory

Evapotranspiration Rates in a Coast Redwood Forest Shelby. *Ecohydrology* e2404 (2022). doi:https://doi.org/10.1002/eco.2404
25. De Lombaerde, E., Verheyen, K., Van Calster, H. & Baeten, L. Tree regeneration responds more to shade casting by the overstorey and competition in the understorey than to abundance per se. *For. Ecol. Manage.* **450**, (2019).
26. Gasperini, C. *et al.* Edge effects on the realised soil seed bank along microclimatic gradients in temperate European forests. *Sci. Total Environ.* **798**, (2021).
27. Potter, K. A., Woods, A. H. & Pincebourde, S. Microclimatic challenges in global change biology. *Glob. Chang. Biol.* **19**, 2932–2939 (2013).
28. Hylander, K., Ehrlén, J., Luoto, M. & Meineri, E. Microrefugia: Not for everyone. *Ambio* **44**, 60–68 (2015).
29. De Pauw, K. *et al.* Forest understorey communities respond strongly to light in interaction with forest structure , but not to microclimate warming. *New Phytol.* **233**, 219–235 (2022).
30. De Frenne, P. *et al.* Light accelerates plant responses to warming. *Nat. Plants* **1**, 4–6 (2015).
31. Govaert, S. *et al.* Rapid thermophilization of understorey plant communities in a 9 year-long temperate forest experiment. *J. Ecolgy* 1–14 (2021). doi:10.1111/1365-2745.13653
32. De Frenne, P. *et al.* Forest microclimates and climate change: Importance, drivers and future research agenda. *Glob. Chang. Biol.* **27**, 2279–2297 (2021).
33. Senf, C. & Seidl, R. Persistent impacts of the 2018 drought on forest disturbance regimes in Europe. *Biogeosciences* **18**, 5223–5230 (2021).
34. Büntgen, U. *et al.* Recent European drought extremes beyond Common Era background variability. *Nat. Geosci.* (2021). doi:10.1038/s41561-021-00698-0
35. Elith, J. *et al.* A statistical explanation of MaxEnt for ecologists. *Divers. Distrib.* **17**, 43–57 (2011).
36. Merow, C. *et al.* On using integral projection models to generate demographically driven predictions of species ' distributions : development and validation using sparse data. *Ecography (Cop.).* **37**, 1167–1183 (2014).
37. Merow, C., Treanor, S., Allen, J. M., Xie, Y. & Silander Jr, J. A. Climate change both facilitates and inhibits invasive plant ranges in New England. *PNAS* 3276–3284 (2017). doi:10.1073/pnas.1609633114
38. Hargreaves, A. L., Samis, K. E. & Eckert, C. G. Are Species' Range Limits Simply Niche Limits Writ Large? A Review of Transplant Experiments beyond the Range. *Am. Nat.* **183**, 157–173 (2014).
39. Lee-Yaw, J. A. *et al.* A synthesis of transplant experiments and ecological niche models suggests that range limits are often niche limits. *Ecol. Lett.* **19**, 710–722 (2016).
40. Dunne, J. A., Saleska, Scott, R., Fischer, M. L. & Harte, J. Integrating experimental and gradients methods in ecological climate change research. *Ecology* **85**, 904–916 (2004).
41. Verheyen, K., Honnay, O., Motzkin, G., Hermy, M. & Foster, D. R. Response of forest plant species to land-use change.pdf. *J. Ecol.* **91**, 563–577 (2003).
42. Easterling, M. R., Ellner, S. P. & Dixon, P. M. Size-specific sensitivity: Applying a new structured population model. *Ecology* **81**, 694–708 (2000).
43. Merow, C. *et al.* Advancing population ecology with integral projection models: a practical guide. *Methods Ecol. Evol.* **5**, 99–110 (2014).
44. Darwin, C. *On the Origin of Species By Means of Natural Selection, or the Preservation of Favoured Races in the Struggle For Life*. (John Murray, 1859).
45. Brown, J. H. *Macroecology*. (University of Chicago Press, 1995).
46. Dobzhansky, T. Evolution in the Tropics. (1950).
47. MacArthur, R. H. *Geographical Ecology: Patterns In the Distribution of Species*. (Princeton university press, 1972).
48. Araújo, M. B. & Luoto, M. The importance of biotic interactions for modelling species

distributions under climate change. *Glob. Ecol. Biogeogr.* **16**, 743–753 (2007).
49. Louthan, A. M., Doak, D. F. & Angert, A. L. Where and When do Species Interactions Set Range Limits? *Trends Ecol. Evol.* **30**, 780–792 (2015).
50. Wisz, M. S. *et al.* The role of biotic interactions in shaping distributions and realised assemblages of species: implications for species distribution modelling. *Biol. Rev.* **88**, 15–30 (2013).
51. Lembrechts, J. J., Nijs, I. & Lenoir, J. Incorporating microclimate into species distribution models. *Ecography (Cop.).* **42**, 1267–1279 (2019).
52. Elemans, M. Light , nutrients and the growth of herbaceous forest species. *Int. J. Ecol.* **26**, 197–202 (2004).
53. Senf, C. & Seidl, R. Mapping the forest disturbance regimes of Europe. *Nat. Sustain.* **4**, 63–70 (2021).
54. Hartmann, H. *et al.* Climate Change Risks to Global Forest Health: Emergence of Unexpected Events of Elevated Tree Mortality Worldwide. *Annu. Rev. Plant Biol.* **73**, 1–30 (2022).
55. Christiansen, D. M., Lønsmann, L., Johan, I. & Hylander, K. Changes in forest structure drive temperature preferences of boreal understorey plant communities. *J. Ecolgy* **110**, 631–643 (2022).
56. Bertrand, R., Aubret, F., Grenouillet, G., Ribéron, A. & Blanchet, S. Comment on "Forest microclimate dynamics drive plant responses to warming". *Science (80-.).* **3850**, 1–4 (2020).
57. Norris, J. R. *et al.* Evidence for climate change in the satellite cloud record. *Nature* **536**, 72–75 (2016).
58. Olson, D. M. *et al.* Terrestrial Ecoregions of the World: A New Map of Life on Earth. *Bioscience* **51**, 933–938 (2001).

Methods

1. Study region

The study region encompasses all forested area within a broad window around the European temperate broadleaf and mixed forest biome[58], between 10°W - 20°E and 40°N - 61°N (Fig. 1).

2. Study species

Twelve species were selected based on their common occurrence in the understorey of temperate European forests and their difference in affinity to light and warmth (*Anemone nemorosa, Oxalis acetosella, Carex sylvatica, Vinca minor, Poa nemoralis, Allium ursinum, Deschampsia cespitosa, Geranium sylvaticum, Geranium robertianum, Geum urbanum, Alliaria petiolata* and *Urtica dioica*). The species' light preference was inferred from the Colonization Capacity Index (CCI)[41], a continuous gradient from -100 (generalist species) to +100 (typical forest specialist species) representing their association with ancient, structurally complex forests (Supplementary Table 1). The CCI generally coincides with the forest specialist – generalist spectrum[41]. For one species (*Geranium sylvaticum*), the CCI was inferred based on expert knowledge because no value was available. The species' warmth preferences were inferred from their Thermal Niche Optimum (TNO), which were calculated as the mean annual temperature within the species' distribution range[59]. Using the species' temperature and light preferences, the species were categorized in four ecological groups: cold-adapted forest specialists; warm-adapted forest specialists; cold-adapted forest generalists and warm-adapted forest generalists.

3. Transplant experiment

A large-scale transplant experiment was installed in early Spring 2019 in five regions along a *c.* 1,750 km long transect spanning the entire European temperature broadleaved forest biome[29] (Fig. 1a). In each region, four experimental locations were established with contrasting forest structure (simple *vs.* dense) and distance to the forest edge (edge *vs*. core; Fig. 1b), hereby capturing a major part of the natural variation in macroclimate, microclimate and light availability in European broadleaf forests. Dense forest stands typically had a well-developed shrub and tree layer, high basal area and canopy cover. Simple forest stands were characterized by a high canopy openness and the absence of a shrub layer. In each forest stand, experimental plots were installed at *c*. 2 m from the south-facing forest edge and in the forest core (minimal distance of 50 m from any forest edge). In total, 20 experimental sites (5 regions × 2 forest types × 2 sites per forest type) were established.

In three regions (Italy, Belgium and South Sweden), experimental heating and irradiance treatments were applied in a full-factorial design (Fig. 1c, Extended Data Fig. 1). Hence, in these regions, each site contained four experimental plots: heating, lighting, heating and lighting, and a control. The experimental sites in France and Central Sweden contained only control plots. In total, the transplant experiment consisted of 56 experimental plots. The experimental treatments were applied during the growing season for three consecutive years, from May 2019 (after installation) till 30 September 2019 and from 1 February till 30 September in 2020 and 2021. More detail on the experimental design are provided in Supplementary Methods 1.

All experimental plots contained nine mesocosm communities, each composed of four individuals (replicates) of four different species (one from each of the two ecological groups, see study species) randomly planted in a rectangular grid of 4 × 4 (27 cm × 37 cm; Fig. 1d, e). The

four species were sampled from the set of twelve species in a stratified way that ensured a combination of one species from each ecological group in each mesocosm, with all species occurring in equal numbers at the plot level. In total, at the onset of the transplant experiment, it contained 8,064 individuals (56 experimental plots × 9 mesocosms × 4 species × 4 individuals) and 672 individuals per species (12 replicates × 56 experimental plots). All biological material originated from the same source in Belgium or Germany to minimize potential effects of local adaptation (Supplementary Table 1).

4. Plant demographic data

Demographic data were collected at the individual plant level (Extended Data Fig. 2). Summer-flowering plant species were measured in July 2019, 2020 and 2021. Spring-flowering plant species were measured in April and May 2020 and 2021. For all species, we measured survival, natural plant height (distance between the soil surface and the uppermost photosynthetic tissue[60]), flowering status and the number of flowers. For *Anemone nemorosa* and *Geum urbanum*, we additionally counted the number of seeds (when present) in 2021. For *Alliaria petiolata* and *Allium ursinum* we measured the seedling size (natural height) in 2021 at the plot level (since parent plants were not exactly known). See Extended Data Fig. 3 for details on the annual sampling sizes.

5. Environmental data

We quantified the environment based on large-scale macroclimate conditions and local-scale variation in forest microclimates and forest density. Five variables were selected that capture major non-edaphic environmental axes in European temperate forest systems at both large- and

small-spatial gradients, and that are potential drivers of plant demography: average growing season temperature; cumulative growing season precipitation; winter and summer temperature offset due to canopy cover and distance to the forest edge; and forest density (supplementary Table 2)[19,29]. Each variable was assessed at the level of the experimental site (for use in the vital rate models and IPMs), and retrieved as raster grids at the extent of the study region (for use in the DDMs) (see Extended Data Fig. 2 for a flowchart of the data).

5.1. Environment of the experimental sites

The *average growing season temperature* and *cumulative growing season precipitation* were calculated as the average of monthly mean growing season (April till July) temperatures and as the sum of monthly mean growing season cumulative precipitation for the most recent available 30-year period (1970-2000) extracted at 30 arcsec (~1 km) resolution from WorldClim v2.1 [projection EPSG:4326][61].

Winter and summer temperature offset values were calculated as subcanopy microclimate temperatures minus macroclimate temperatures. The winter offset metric positively relates to the capacity of canopies to buffer free-air thermal minima and increased with forest structure and distance to the forest edge. The summer offset metric negatively relates to the capacity of canopies to buffer free-air thermal maxima and decreases with forest structure and distance to the forest edge[19,21]. *In situ* microclimate temperatures were measured at 15 cm above the soil surface using TMS-4 loggers (TOMST, Prague, Czech Republic) installed in the centre of each control plot (n = 20), and covered by a white radiation shield. Local air temperatures were recorded at 15 min intervals from 17 May 2019 till 30 June 2021. Hourly mean microclimate temperatures were calculated to match the temporal resolution of the macroclimate data. Hourly mean macroclimate

511 temperatures at 2 m height for each control site were extracted from the ERA5-land reanalysis
512 data base[62] at the spatial resolution of 0.1 × 0.1 degrees (native resolution of 9 km) [EPSG:4326].
513 Hourly offset values (ΔT °C) were calculated as microclimate minus macroclimate temperatures.
514 Finally, for each experimental site, summer offsets were calculated as the average offset from
515 June till August. Winter offsets were calculated as the average offset from December till
516 February.
517 *Forest density* was quantified as the cumulative percentage of tree canopy cover and shrub cover
518 within a circle with radius of 9 m around the centre of each experimental site. The cumulative
519 percentage was standardized to a maximum of 100%.
520
521 5.2. Environmental data of the study area
522 Gridded *average growing season temperature* and *cumulative growing season precipitation* data
523 were calculated as the average of monthly mean growing season temperatures and as the sum of
524 monthly mean growing season cumulative precipitation for the most recent available 30-year
525 period (1970-2000) at 30 arcsec (~1 km) resolution from WorldClim v2.1 [EPSG:4326] and
526 projected to an equal area projection [EPSG:3035].
527 Gridded *summer temperature offset* data were calculated as the average offset from June till
528 August. Gridded w*inter temperature offset* data were calculated as the average offset from
529 December till February. Gridded Monthly temperature offset data were retrieved from Haesen et
530 al., (2021)[20] at the resolution of 25 m [EPGS:3035].
531 Gridded *forest density* data were retrieved from the 2015 Copernicus tree cover density map and
532 represent the average horizonal tree cover density (in a range of 0 - 100 %;
533 https://land.copernicus.eu/pan-european/high-resolution-layers/forests/tree-cover-density/status-

maps/2015) in a grid of 20 × 20 m [EPSG:3035]. Gridded forest density data were resampled to 25 m resolution using a bilinear interpolation.

5.3. Future environmental data

The future *average growing season temperature* and *cumulative growing season precipitation* for the period 2070 (i.e. average for the period 2061 – 2080) were retrieved from WorldClim v2.1 under phase 5 of the Coupled Model Intercomparison Project (CMIP5) at 30 arcsec resolution for the representative concentration pathway RCP8.5. Gridded future average growing season temperature (mean of monthly maximum and minimum temperatures) and cumulative precipitation data were calculated as averages across four General Circulation Models (GCMs) to consider uncertainty related to each GCM. The GCMs were selected based on minimal interdependency following[63] and data availability in WorldClim v2.1. We included MIROC5, INMCM4, ACCESS1-0 and CNRM-CM5.

To evaluate the effects of forest management (and hence changes in forest structure) on population dynamics, two additional *forest cover density* maps with a hypothetical decrease and increase of 50% forest cover density (always with a maximum of 100%) were simulated. A decrease of 50% in forest density in response to management or natural disturbance is a realistic scenario: the average disturbance severity in European disturbed forest patches is 77% (with 0% indicating zero loss and 100% indicating complete replacement)[53].

For the sake of simplicity, we assumed temperature offset values to stay constant over time although macroclimate warming might enhance offset values[22]. Our estimates are thus conservative.

6. Demographic models

6.1. Vital rate models

Individual-level measurements of six vital rates describing key transitions in the plant's generative life cycle were regressed against experimental site-level environmental data (5.1) and plant size (for implementation in the IPMs) (Fig. S2, S4). The six vital rates included survival probability (n = 12 species), growth rate (n = 12), flowering probability (n = 8), number of reproductive structures (flowers or inflorescences; n = 8), number of seeds per fruit (n = 2) and seedling sizes (n = 5). Vital rates of species with too few or no observations were not modelled and introduced as constant values in the IPMs (Supplementary Tables 1,3).

The vital rates were analysed with mixed-effect models in the R package *lme4*[64] for each species separately. Prior to modelling, the state variable 'plant size' was checked for normality based on visual inspection and transformed (*ln* or *sqrt*) when appropriate (Supplementary Table 1, Extended Data Fig. 5). To account for the nested experimental design, 'mesocosm ID' (9 levels) was included as random intercept in all models of vital rates that were measured at the level of the individual. As a sensitivity analysis against this approach, we also tested an alternative random effect term accounting for the fully nested study design: 'mesocosm ID' nested within 'experimental site' nested within 'forest type' nested within 'region'. This, however, did not changed the general trends in parameter estimates of the fixed effects (Extended Data Fig. 6). We therefore opted to keep the simpler random structure in all models. To account for environmental stochasticity across the study period, 'sampling year' was included as an additional random intercept in all vital rates models that were measured for more than one annual transition. Growth rate and the seedling size were regressed with linear mixed models (LMMs).

Survival and flowering probability (binary distributed) were regressed with generalized linear mixed-effect models (GLMMs) and a binomial error distribution. The number of reproductive structures and the number of seeds were regressed with GLMMs and a Poisson error distribution. The vital rate models included plant size (when relevant) and all environmental variables as fixed effect terms. Pairwise spearman correlations (r) among the environmental variables were acceptable (median $|r| = 0.17$; maximum $|r| = 0.62$)[65]. The seedling size models of *Alliaria petiolata* and *Allium ursinum* and the seed number models did not include the macroclimate predictors to avoid over-extrapolation because these vital rates were only measured in the sites of Belgium and Sweden[66]. The optimal level of model complexity was evaluated based on the lowest Akaike information criterion with small-sample correction (AICc) by comparing all possible nested models with reduced complexity using the R package *MuMIn*[67]. For the model selection of the LMMs growth rate and the seedling size, we first set the restricted maximum likelihood (REML) argument to "FALSE". Once the best model structure was selected, we set REML to TRUE for exact coefficient estimation[64]. Model fit of the selected models was assessed as the percentage of variance explained by the fixed effects (marginal R^2; R^2_m), and the percentage of variance explained by both fixed and random effects (conditional R^2; R^2_c) following Nakagawa & Schielzeth (2013)[68]. We only tested linear responses of the vital rates to the environmental gradients and plant size. Nevertheless, we also performed a qualitative sensitivity analyses against this approach by fitting the vital rate models with more flexible Generalized Additive Models (GAMs; details in Supplementary Methods 2; Extended Data Fig. 7).

To analyse the relation between the species association with ancient forests (inferred from the CCI) and the responses of the survival probability to changes in the environment, we ran linear models with the parameter coefficients of this vital rate model as response variable, and the species' CCI as predictor. The linear models were ran in a Bayesian framework using the R package *brms*[69] that allows to take the standard errors around the model coefficient estimates into account. We used default chain parameters.

6.2. Integral Projection Models (IPMs)

The effects of the environment and experimental treatments on population growth rates (λ) were investigated by combining the vital rate models (as built in section 6.1) into Integral Projection Models (IPMs[42]). IPMs are analogous to matrix population models that allow the integration of multiple vital rates regressed against a continuous state variable, and are well-suited to gain mechanistic understanding on population dynamics to changes in the environment by including environmental covariates into each vital rate model of the IPM[43]. We built IPMs based on 'plant height' (sqrt- or ln-transformed; see 6.1) as the continuous state variable. For biennial species (*Geranium robertianum* and *Alliaria petiolata*), IPMs included 'age' as an additional state variable to explicitly account for their biennial life cycle[70,71]. We did not construct IPMs (and DDMs) for *Vinca minor*, *Geranium sylvaticum* and *Oxalis acetosella* due to the absence of fecundity data in these species. For these species, responses to the environment were only inferred based on the vital rates survival probability and growth rate.

Because we could not infer vital rates related to vegetative reproduction (clonal growth) due to the lack of empirical data (this would require destructive sampling), the approach presented here

estimates population growth rates that apply on generative population growth in the phase of population establishment. Nevertheless, we acknowledge that for some forest plants, vegetative reproduction is an important aspect of the life cycle. In addition, the estimated λ implicitly accounts for the effects of neighbouring competitors as all individuals were transplanted into community mesocosms. Details on the IPM structure are described in Supplementary Methods 3.

6.3. Demographic Distribution Models (DDMs)

6.3.1. Demography-based distribution maps (i.e. maps of λ)

Demography-based distribution maps (i.e. maps of λ) for each species were produced by projecting the IPMs across the study extent[36,37] (Extended Data Fig 2). Both continental- and landscape-scale maps were produced to assess the model's behaviour along macro- and microclimate gradients. Continental-extent maps were computed by iterating the IPM for each species in 1,000,000 random forested locations sampled within the study area. IPMs in these locations were supplied with environmental covariate values extracted from the 25-m resolution environmental layers. Landscape-extent maps were computed by iterating the IPM in all forested 25 × 25 m cells in a squared area of 2 × 2 km (400 ha) around the centroid of the experimental plots in Italy, Belgium and South Sweden. Hence, both continental-extent and landscape-extent maps relied on 25 meter resolution environmental data. Projected maps of λ were computed for the current environmental conditions and all combinations of future macroclimate change and a 50% increase or decrease in forest cover density.

In all model future scenarios, we assumed temperature offsets to stay constant over time although forest disturbance reduces offset values[19,21] and warming enhances offset values under maintained forest cover[22]. The rationale behind this decision was two-fold: (1) projected future

high-resolution below-canopy temperature offset data at the European scale are simply not yet available to date; (2) using constant temperature offset values under different forest management and climate-change scenarios allowed us to isolate the effect of changes in species' demography within the community driven by the independent effect of light[30].

The effects of the experimental heating and irradiation treatments on the intercepts of the vital rates were not included in the future DDM predictions. Hence, we applied a *space-for-time* substitution to make future predictions, i.e. we only used the spatial gradient from the transplant experiment to infer changes over time, not including the temporal change brought on by the experimental treatments. All DDM predictions implicitly included forest edge effects by the vital rate responses to less buffered microclimates and more light availability that are typical for forest edges[21,72].

Geographic uncertainty of population growth rates (λ) was quantified by bootstrapping (Supplementary Methods 4).

Parallel computation was implemented using the R packages *foreach*[73] and *doParallel*[74]. Maps were produced using the R package *tmap*[75], and are in an equal area projection [EPSG:3035]. In all maps, λ values higher than the 97.5% quantile were projected to the 97.5% quantile to avoid extremely high λ values in response to marginal environments that obscure the main gradient of the maps.

6.3.2 Scenario analyses under variable forest cover density

To quantify the impact of variable forest cover density (e.g. in response to changes in the forest management), we calculated the population growth rate in a subset of 10,000 random locations under all combinations of current and future climatic conditions and an increased and decreased

forest cover density of 10%, 20%, 30%, 40%, and 50%. The proportional change (relative the population growth rate under the baseline climate and forest cover conditions) was calculated and plotted for each species.

6.3.3 Validation of the distribution maps

A general and convenient method to validate DDM predictions is currently not existing. We here developed a method to test whether the DDMs perform better than random based on a quantitative comparison of the average population growth rates in occurrence locations (i.e. locations were the species was observed) *versus* random background locations. The average population growth rates in occurrence locations are expected to be higher compared to the background locations if a model is better than random. Significant differences between the two groups were tested with one-sample t-tests. Occurrence locations for each species were extracted from the Global Biodiversity Information Facility (GBIF, http://www.gbif.org). To improve the data quality, all occurrence locations were subject to a systematic cleaning protocol (Supplementary Methods 5). Unfortunately, we could not collect enough 'real' absence data points for all species, and therefore had to work with background locations as an alternative. At these background locations, the target species could be either absent or unobserved.

For each species, population growth rates were calculated for 1,000 forested occurrence locations and 1,000 forested background locations. Because the median coordinate uncertainty of the cleaned occurrence locations after cleaning was still relatively low (333 meter), we calculated the population growth rate as the average population growth rate of all raster cell within an area of ~1 km² (i.e. circular area with a radius of 564 meter) around these locations. Additional details are provided in Supplementary Methods 6.

All analyses were performed in R version 4.1.0[76].

Data availability

Macroclimate data are available through the global climate archive WorldClim (https://www.worldclim.org/data/index.html). Spatial temperature offset data between forest and open field conditions are available at https://doi.org/10.6084/m9.figshare.14618235[20]. Tree cover density data are available at https://land.copernicus.eu/pan-european/high-resolution-layers/forests/tree-cover-density/status-maps/2015. Georeferenced observation records used for the continental scale validation of the Demographic Distribution Models (DDMs) are available at https://doi.org/10.15468/dl.3nvzc8 All experimental plant demographic data and site-level environmental data will be made available on an online repository such as FigShare (https://figshare.com/) (temporary private link to the data is already available: https://figshare.com/s/35b070818230ce5795d3).

Code availability

All scripts to reproduce the methods, analyses and figures will be made available on an online repository such as FigShare (https://figshare.com/) (temporary private link to the code to the code: https://figshare.com/s/35b070818230ce5795d3).

Acknowledgements

We thank Kris Ceunen, Hans Rudolf Schaffner, Ulf Johansson, Sarah Vaneenooghe, Jonathan Van Loo, Sam Van Bouchaute, Linnea Glav Lundin, Tom Augustijns and Stef Haesen for fieldwork and technical assistance.

Funding: This work was supported by the European Research Council (ERC) (ERC Starting Grant FORMICA 757833, 2018, http://www.formica.ugent.be); the Research Foundation

718 Flanders (FWO) (K.D.P. ASP035-19, S.G. G0H1517N), and the FWO Scientific research
719 network FLEUR (http://www.fleur.ugent.be).

720

721 **Author contributions**

722 PS, KDP, EDL, ML, KV, PV and PDF conceived the ideas and designed methodology; all
723 authors collected data; PS analysed data in collaboration with EDL, ML, PV and PDF; PS led the
724 writing of the manuscript in collaboration with KDP, ED, PV and PDF. All authors contributed
725 critically to the draft and gave final approval for publication.

726

727 **Competing interests**

728 None of the authors have a conflict of interest

Methods references

59. Vangansbeke, P. *et al.* ClimPlant : Realized climatic niches of vascular plants in European forest understoreys. *Glob. Ecol. Biogeogr.* **30**, 1183–1190 (2021).
60. Pérez-Harguindeguy, N. *et al.* New handbook for standardised measurement of plant functional traits worldwide. *Aust. J. Bot. 6* **20**, 715–716 (2016).
61. Fick, S. E. & Hijmans, R. J. WorldClim 2: new 1-km spatial resolution climate surfaces for global land areas. *Int. J. Climatol.* (2017). doi:10.1002/joc.5086
62. Muñoz-sabater, J. *et al.* ERA5-Land: A state-of-the-art global reanalysis dataset for land applications. *Earth Syst. Sci. Data Discuss.* 1–50 (2021). doi:https://doi.org/10.5194/essd-2021-82
63. Sanderson, B. M., Knutti, R. & Caldwell, P. A Representative Democracy to Reduce Interdependency in a Multimodel Ensemble. *J. Clim.* **28**, 5171–5194 (2015).
64. Bates, D., Mächler, M., Bolker, B. M. & Walker, S. C. Fitting Linear Mixed-Effects Models Using lme4. *J. Stat. Softw.* **67**, 1–29 (2015).
65. Dormann, C. F. *et al.* Collinearity : a review of methods to deal with it and a simulation study evaluating their performance. *Ecography (Cop.).* **27**, 27–46 (2013).
66. Fernández-Fernández, P. *et al.* Different effects of warming treatments in forests versus hedgerows on the understorey plant Geum urbanum. *Plant Biol.* (2022). doi:https://doi.org/10.1111/plb.13418
67. Barton, K. MuMIn: Multi-Model Inference. (2017).
68. Nakagawa, S. & Schielzeth, H. A general and simple method for obtaining R 2 from generalized linear mixed-effects models. **2**, 133–142 (2013).
69. Bürkner, P. Bayesian Item Response Modeling in R with brms and Stan. *J. Stat. Softw.* **100**, 1–54 (2021).
70. Childs, D. Z., Rees, M., Rose, K. E., Grubb, P. J. & Ellner, S. P. Evolution of complex flowering strategies: an age- and size-structured integral projection model. *Proc. R. Soc. B* **270**, 1829–1838 (2003).
71. Ellner, S. P. & Rees, M. Integral Projection Models for Species with Complex Demography. *Am. Nat.* **167**, 410–428 (2006).
72. Meeussen, C. *et al.* Structural variation of forest edges across Europe. *For. Ecol. Manage.* **462**, 117–929 (2020).
73. Microsoft & Weston, S. foreach: Provides Foreach Looping Construct. (2020).
74. Microsoft & Weston, S. doParallel: Foreach Parallel Adaptor for the 'parallel' Package. (2020).
75. Tennekes, M. *et al.* tmap: Thematic Maps. *J. Stat. Softw.* **84**, 1–39 (2018).
76. R Core Team. *A language and environment for statistical computing. R Foundation for Statistical Computing*. (2021).